Applied Energy 230 (2018) 277–286

Contents lists available at ScienceDirect

Applied Energy

journal homepage: www.elsevier.com/locate/apenergy

Investments in merchant energy storage: Trading-off between energy and reserve markets

H. Pandžić[a,*], Y. Dvorkin[b], M. Carrión[c,1]

[a] Faculty of Electrical Engineering and Computing University of Zagreb, Unska 3, Zagreb, Croatia
[b] Department of Electrical and Computer Engineering at New York University, New York, NY, USA
[c] School of Industrial Engineering, University of Castilla-La Mancha, Toledo, Spain

HIGHLIGHTS

- Joint energy and reserve market increases energy storage profits.
- Revenue collected by energy storage in reserve market is lower than in energy market.
- Storage siting and sizing and its profitability depend on transmission line limits.

ARTICLE INFO

Keywords:
Energy storage
Day-ahead market
Reserve market
Bilevel program

ABSTRACT

Grid-scale energy storage units are regarded as an enabler of the renewable-dominant power systems. Currently available energy storage technologies are ubiquitous, but not equally suitable for providing different grid support services. As part of their investment process, merchant energy storage investors need to ensure that their energy storage investments are well aligned with unique grid support needs of each power system and that the storage characteristics are suitable for the simultaneous provision of multiple services.

This paper presents a model to optimize merchant investments in energy storage units that can compete in the joint energy and reserve market. The proposed model uses the bilevel programming framework to maximize the expected lifetime profit and to ensure a desirable rate-of-return for the merchant energy storage investor, while endogenously considering market clearing decisions over a set of characteristic days. The bilevel model is first converted into a single-level equivalent using the Karush-Kuhn-Tucker-based approach and then linearized to obtain a mixed-integer linear program. The resulting program is solved using the Benders' decomposition approach and tested on the 8-zone Independent System Operator New England test system. The case study provides numerical insights that are discussed from viewpoints of the merchant energy storage owner, the system operator, and the regulator.

1. Introduction

Following an extensive deployment of renewable generation resources, there is a pressing need to maximize their available power output and thus their economic value to power systems. This task entails dealing with two most urgent issues. First, one needs to mitigate the impact of these resources on power system operations due to their inherent uncertainty and variability. Second, there is a need to synchronize weakly correlated demand and renewable generation profiles. Both issues can effectively be overcome by installing grid-scale energy storage (ES) units, [1,2]. As flexible resources, ES units can provide reserve and thus mitigate the impact of the uncertainty and variability of renewable generation resources. Furthermore, ES units can perform spatio-temporal energy arbitrage, [3], by accommodating the surplus renewable generation and storing it for later use, thus increasing utilization of the available renewable generation. The simultaneous use of ES units for reserve provision and spatio-temporal energy arbitrage requires a strict distinction between the ES power and energy capacity to provide these services in a physically and economically feasible manner. The ability of ES units to provide different services and, hence, its value to the power system depend on their technology-specific capabilities, which need to be examined thoroughly before investing in

* Corresponding author.
E-mail addresses: hrvoje.pandzic@fer.hr (H. Pandžić), yvd204@nyu.edu (Y. Dvorkin), Miguel.Carrion@uclm.es (M. Carrión).
[1] The authors contributed equally and their names are ordered counter-alphabetically.

https://doi.org/10.1016/j.apenergy.2018.08.088
Received 22 April 2018; Received in revised form 28 July 2018; Accepted 16 August 2018

Nomenclature

Sets and indices

B	set of buses, indexed by b
E	set of characteristic days, indexed by e
I/I_b	set of generators/subset of generators connected to bus b, indexed by i. Note that $I_b \subseteq I$
L	set of transmission lines, indexed by l
T	set of time intervals, indexed by t
$\Xi_{[\cdot]}$	set of decision variables. Subscript $[\cdot]$ denotes upper-level (UL), lower-level (LL), and dual lower-level (DLL)
$o(l)$, $r(l)$	indices of sending and receiving ends of line l.

Constants

$C^{\text{SoC}}/C^{\text{P}}$	annualized capital cost of ES per kWh (\$/kWh)/per kW (\$/kW)
C_i^{g}	energy price offered by generator i, \$/MWh
$C_i^{\text{g},\uparrow/\downarrow}$	price offered by generator i to provide up/down reserve, \$/MWh
$C_b^{\text{ch/dis}}$	charging/discharging energy price bid/offer of ES at bus b, \$/MWh
$C_b^{\text{ES},\uparrow/\downarrow}$	price offered by ES at bus b to provide up/down reserve, \$/MW
D_{etb}	demand at bus b during interval t on characteristic day e, MW
$\overline{G}_i$	maximum power offered by generator i, MW
$\overline{P}_l^{\text{f}}$	power flow limit in transmission line l, MW
$IC^{\max}$	annualized investment budget, \$
RU_i/RD_i	ramp up/down limit of generator i, MW/h
P_{etb}^{wf}	forecast wind power offer at bus b during interval t on characteristic day e, MW
$R_{et}^{\text{UP}}/R_{et}^{\text{DN}}$	up/down reserve requirements during interval t on characteristic day e, MW
$\overline{R}_{eti}^{\text{g},\uparrow/\downarrow}$	maximum up/down reserve by generator i during interval t on characteristic day e, MW
X_l	reactance of line l
Δ	duration of the dispatch interval
$\aleph^{\text{ch}}/\aleph^{\text{dis}}$	charging/discharging efficiencies of ES
γ^{EP}	energy/power ratio of ES
γ_0	state of charge of ES at the beginning of each characteristic day, pu
μ	minimum ES state of charge, pu
π_e	weight of characteristic day e
τ	duration of reserve provision, h
χ	parameter setting the minimum return-on-investment of ES investor.

Continuous variables

ch_{etb}/dis_{etb}	ES charging/discharging market–cleared quantities at bus b during interval t on characteristic day e, MW
$\overline{ch}_{etb}/\overline{dis}_{etb}$	charging/discharging quantities offered by ES at bus b during interval t on characteristic day e, MW
SoC_{etb}	state of charge of ES at bus b at the end of interval t on characteristic day e, MWh
$SoC_b^{\max}$	maximum state of charge of ES at bus b, MWh
p_{etl}^{f}	power flow through line l during interval t on characteristic day e, MW
p_{eti}^{g}	power output of generator i during interval t on characteristic day e, MW
$r_{eti}^{\text{g},\uparrow/\downarrow}$	up/down reserve provided by generator i during interval t on characteristic day e, MW
$r_{etb}^{\text{ES},\uparrow/\downarrow}$	up/down reserve market-cleared quantities provided by ES at bus b during interval t on characteristic day e, MW
$\overline{r}_{etb}^{ES,\uparrow/\downarrow}$	up/down reserve quantities offered by ES at bus b during interval t on characteristic day e, MW
$\overline{r}_{etb}^{\text{ch},\uparrow/\downarrow}$	up/down reserve quantities offered by ES in charging mode at bus b during interval t on characteristic day e, MW
$\overline{r}_{etb}^{\text{dis},\uparrow/\downarrow}$	up/down reserve quantities offered by ES in discharging mode at bus b during interval t on characteristic day e, MW
IC	ES investment cost, \$
$P^{\text{E}}/P^{\text{R}}$	ES profit in energy/reserve markets, \$
$p_b^{\max}$	power charging/discharing rating of ES at bus b, MW
p_{etb}^{ws}	wind spillage at bus b during interval t on characteristic day e, MW
θ_{etb}	voltage phase angle at bus b during interval t on characteristic day e, rad

and rolling-out these units in real-life systems [4].

Physical feasibility is necessitated by the energy-limited nature of ES units. In other words, the arbitrage and reserve allocations need to be coordinated to avoid depleting stored energy and failing to deliver one or more services as scheduled. Economic feasibility is motivated by the need to weigh profit opportunities in the energy and reserve markets. The relative proportion of revenue streams available to ES units in the energy and reserve markets will affect the willingness of the merchant investor to invest in ES units and will have a bearing on the optimal ES siting and sizing decisions. Analyzing the trade-off between the energy and reserve markets is of great importance in the context of the existing wholesale markets as merchant ES units can significantly influence market outcomes [5]. From the merchant perspective, it is important to balance participation of their ES units in the energy and reserve markets and foresee the impacts of high penetration levels of renewable generation resources. Integration of renewable generation resources tends to reduce the average wholesale energy prices, while increasing the need for and the price of reserve services. Relationship between the energy and reserve prices in systems with high penetration of renewable generation resources, as well as its impact on the ES siting and sizing decisions, is not straightforward, but can endogenously be accounted for if the ES siting and sizing decisions are considered with respect to the market clearing procedures. Furthermore, unlike conventional generation resources, ES units are better suited for exercising market power as they can act as both consumers and producers, thus creating more opportunities to influence market outcomes in their self-interest. Therefore, the ability to act strategically must also be factored in the investment optimization process of the ES investor.

Previously, optimal investments in ES units have been studied from the vertically integrated [3,6–10], merchant [5,11–15] or hybrid [16] perspectives. The models in [3,6–10] aim to find storage siting and sizing decisions that maximize the expected operating cost savings over a set of characteristic operating conditions represented by exogenous load and renewable power output profiles. From the modeling perspective, [3,6–10] formulate a two-stage mixed-integer linear program (MILP). In these models, the first stage optimizes the ES investment decisions. The second stage co-optimizes operating decisions on the existing generation resources and ES units installed in the first stage over a set of characteristic operating conditions. However, as numerically shown in [10], models in [3,6–10] tend to result in ES siting and sizing decisions that yield insufficient lifetime profits to justify the merchant investment. The model in [5] overcomes this limitation by exploiting the bilevel programming framework that endogenously enforces a lower bound on the expected lifetime profit of the ES units. The same modeling framework is used in [14,15], which study the impact of demand response resources and transmission expansion decisions on the merchant ES investments. In [17], the ES and transmission expansion co-optimization is also complemented by accounting the effects of demand-side management resources. The models in [11,12] also use the bilevel programming framework, but ignore the transmission network limits and, therefore, optimize the ES sizing decisions only. As discussed in [5], ignoring network constraints can miscalculate the expected lifetime profit of merchant ES units and limit their value to the power system. To convert the original models into a single-level equivalent in [5,11–16], the authors use either the Karush-Kuhn-Tucker (KKT) optimality conditions or duality-based approach. The equivalent problem is a MILP that can be solved using off-the-shelf solvers, [5,14], Benders' decomposition, [11,12], or constraint-and-column generation, [15,16]. The common thread of studies in [5,11–16] is that they ignore revenue streams available to the merchant ES units in the reserve market. As power systems transition toward the renewable-dominant power supply, the role and volume of the reserve market is expected to increase and lead to profit opportunities comparable to the energy market [18]. In turn, this shift toward the reserve market can affect optimal siting and sizing decisions of merchant ES units as the energy and reserve markets may benefit from different ES performance characteristics.

The common thread of the studies in [3,5–16] is that they use the net present value approach and do not internalize the long-term uncertainty and perform a sensitivity analysis to reveal impacts of various parameters on the optimal investment parameter. Alternatively, [19,20] exploit linear decision rules to factor in the long-term uncertainty (e.g. capital cost of new resources, load and generation growth) in a multi-stage stochastic MILP used for power system planning. Additionally, [21] proposes a valuation framework for pumped hydro energy storage investments based on a real option analysis that allows for a more refined treatment of parameters that are subject to long-term uncertainty factors.

Currently, there is no modeling solution that would account for the simultaneous participation of the merchant ES units in the energy and reserve markets, while optimizing the ES investments. This paper addresses this gap and makes the following contributions:

1. It proposes a new model intended for merchant ES investors that optimizes the ES siting and sizing decisions ensuring a desirable rate-of-return during the expected lifetime from the wholesale energy and reserve markets. The proposed model endogenously trades off revenue opportunities in energy and reserves markets. As a result, the optimized ES siting and sizing decisions accurately match the energy arbitrage and reserve needs of the power system.
2. Using the KKT-based method [22], the proposed model is converted into the single-level equivalent as has previously been done in [5,14,15]. Since the proposed model considers both the energy and reserve markets, the single-level equivalent differs from those in [5,14,15] and requires dealing with new nonlinear terms to obtain a MILP. Furthermore, the obtained MILP equivalent cannot be solved using the off-the-shelf solvers for realistically sized instances with a sufficient number of characteristic days. To overcome the computational complexity, Benders' decomposition is applied and the decomposed single-level MILP equivalent is solved iteratively.
3. The case study is carried out on the 8-zone ISO New England test system [23] for different capital cost scenarios of prospective ES technologies. As the capital cost changes, the case study reveals how the optimal ES siting and sizing decisions, as well as the trade-off between the energy and reserve market revenues, shifts. The case study also analyzes the impact of reserve requirements on the ES profitability.

Closest works to this paper are reported in [24,25]. Li and Hedman [24] focus on the economic analysis of ES impacts on power system operations under high penetration levels of renewable generation from the system (vertically integrated) perspective. The model in [24] captures the arbitrage and reserve benefits of ES units. Relative to this paper, [24] does not optimize investment decisions on ES units and does not explicitly ensure profitability of merchant ES units. Similarly to [24,25] takes the system perspective and merely ensures that energy storage units break even during their lifetime, i.e. it does not maximize the ES profit as in this paper and does not internalize strategic behavior. Furthermore, the solution technique in [25] is bound to suffer from a relatively high termination tolerance (e.g. 5%).

The work described in this paper is also timely in light of the recent ES integration projects in the US and Europe, which aim at decarbonizing the power sector [26]. The latter is particularly important as ES units are shown to cause complex impacts on power system dispatch decisions and thus reduce overall emissions [27]. In [28], the authors propose a set of metrics to examine the techno-economic ability of a grid-scale ES to provide different ancillary services. These metrics are then used to seek the best match of ES technologies and ancillary services. In practice, the US Energy Storage Association already counts hundreds of new merchant ES units installed in 2010s [29]. In Europe, battery ES units participate in many wholesale markets with the largest cumulative battery ES capacity in Italy of more than 242 MWh [30]. One part of this storage is *energy intensive*, i.e. with charging/discharging periods up to 6 h, while the other part is *power intensive* with a goal of performing primary frequency regulation. Furthermore, social costs and benefits of a 6MW/10MWh ES in the United Kingdom are quantified using the Monte Carlo simulation framework, which is claimed to result in cost-efficient investments in ES units [31]. These real-life installations illustrate the need for the model proposed in this paper, see [32–34].

2. Bilevel model

The proposed bilevel model is illustrated in Fig. 1. Structurally, this program is somewhat similar to the models in [25,14,5], but is extended to account for the reserve provision and market interactions, which requires a different solution procedure. The upper-level (UL) problem optimizes ES investment decisions ($SoC_b^{\max}$ and $p_b^{\max}$) and the bidding and offering decisions for each characteristic day. The bidding decisions include capacity and price bids to charge ($\overline{ch}_{etb}$, C_b^{ch}) and offers to discharge ($\overline{dis}_{etb}$, C_b^{dis}) in the energy market and provide up ($\overline{r}_{etb}^{\mathrm{ES},\uparrow}$, $C_b^{\mathrm{ES},\uparrow}$) and down ($\overline{r}_{etb}^{\mathrm{ES},\downarrow}$, $C_b^{\mathrm{ES},\downarrow}$) reserve services in the reserve market. The lower-level (LL) problem optimizes bids and offers of the ES investor considering bids and offers of other market participants for each characteristic day and returns the cleared quantities (ch_{etb}, dis_{etb}, $r_{etb}^{\mathrm{ES},\uparrow}$, $r_{etb}^{\mathrm{ES},\downarrow}$) and the energy ($\lambda_{etb}$) and reserve ($\lambda_{et}^{r,\uparrow}$ and $\lambda_{et}^{r,\downarrow}$) prices.

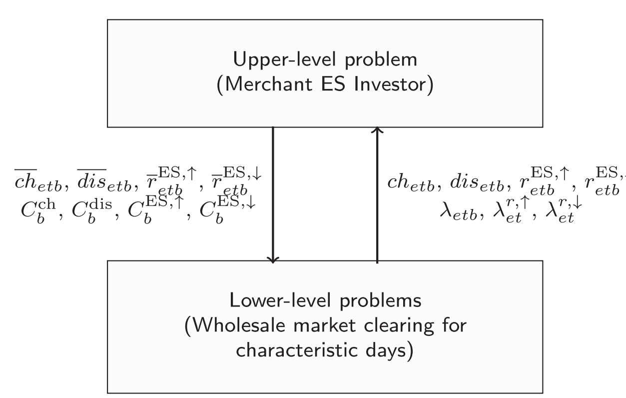

Fig. 1. Illustration of the proposed bilevel model and the interfaces between the upper- and lower-level problems.

2.1. Assumptions

The proposed model invokes the following assumptions:

1. The UL problem takes the viewpoint of a single merchant ES investor (however, the model can be extended to multiple investors, see [14]). The investment decisions are optimized for a target year, while the ES operational decisions are optimized for each characteristic day individually. The investment model assumes a uniform capacity decay during the ES lifetime and zero residual value.
2. The LL problem is a day-ahead wholesale electricity market, which co-optimizes energy and reserve services. Different reserve services (e.g. regulation, load following, contingency reserve) are lumped and represented by a given system-wide deterministic reserve criterion, [35]. Demand is modeled as inelastic.
3. The merchant ES investor is the only strategic participant in the electricity market, while other market participants bid and offer at their marginal cost.
4. Energy is priced on a nodal and hourly basis, i.e. producers and consumers get paid and pay the LMP calculated at the bus where they are located. Transmission network is represented using a lossless dc power flow approximation. Reserve pricing is system-wide and is not differentiated on a nodal basis. Although the proposed model considers nodal energy prices, it can be accommodated to account for zonal and uniform energy prices as practiced in some systems [36].

2.2. UL problem

The merchant ES investor problem is modeled as follows:

$$\max_{\Xi_{\mathrm{UL}}} P^{\mathrm{E}} + P^{\mathrm{R}} - IC \tag{1}$$

subject to:

$$P^{\mathrm{E}} = \sum_{e\in E} \pi_e \sum_{b\in B} \sum_{t\in T} \lambda_{etb}(dis_{etb} - ch_{etb}) \tag{2}$$

$$P^{\mathrm{R}} = \sum_{e\in E} \pi_e \sum_{b\in B} \sum_{t\in T} (\lambda_{et}^{r,\uparrow}\cdot r_{etb}^{\mathrm{ES},\uparrow} + \lambda_{et}^{r,\downarrow}\cdot r_{etb}^{\mathrm{ES},\downarrow}) \tag{3}$$

$$IC = \sum_{b\in B} (C^{\mathrm{SoC}}\cdot SoC_b^{\max} + C^{\mathrm{p}}\cdot p_b^{\max})\cdot K^{\mathrm{e}}\cdot\frac{(1+R)^L}{L} \tag{4}$$

$$IC \leqslant IC^{\max} \tag{5}$$

$$P^{\mathrm{E}} + P^{\mathrm{R}} \geqslant \chi\cdot IC \tag{6}$$

$$SoC_b^{\max} = \gamma^{\mathrm{EP}} p_b^{\max}, \quad \forall\ e, t, b \tag{7}$$

$$SoC_{etb} = SoC_{e,t-1,b} + \Delta(\overline{ch}_{etb}\cdot\aleph^{\mathrm{ch}} - \overline{dis}_{etb}/\aleph^{\mathrm{dis}}), \quad \forall\ e, t, b \tag{8}$$

$$SoC_{etb} + \tau\cdot\overline{r}_{etb}^{\mathrm{ES},\downarrow}\cdot\aleph^{\mathrm{ch}} \leqslant SoC_b^{\max}, \quad \forall\ e, t, b \tag{9}$$

$$SoC_{etb} - \tau\cdot\overline{r}_{etb}^{\mathrm{ES},\uparrow}/\aleph^{\mathrm{dis}} \geqslant \mu\cdot SoC_b^{\max}, \quad \forall\ e, t, b \tag{10}$$

$$SoC_{etb} = \gamma_0 SoC_b^{\max}, \quad \forall\ e, b, t=0 \tag{11}$$

$$SoC_{etb} \geqslant \gamma_0 SoC_b^{\max}, \quad \forall\ e, b, t=24 \tag{12}$$

$$\overline{r}_{etb}^{\mathrm{ES},\uparrow} = \overline{r}_{etb}^{\mathrm{ch},\uparrow} + \overline{r}_{etb}^{\mathrm{dis},\uparrow}, \quad \forall\ e, t, b \tag{13}$$

$$\overline{r}_{etb}^{\mathrm{ch},\uparrow} \leqslant \overline{ch}_{etb}, \quad \forall\ e, t, b \tag{14}$$

$$\overline{r}_{etb}^{\mathrm{dis},\uparrow} \leqslant p_b^{\max} - \overline{dis}_{etb}, \quad \forall\ e, t, b \tag{15}$$

$$\overline{r}_{etb}^{\mathrm{ES},\downarrow} = \overline{r}_{etb}^{\mathrm{ch},\downarrow} + \overline{r}_{etb}^{\mathrm{dis},\downarrow}, \quad \forall\ e, t, b \tag{16}$$

$$\overline{r}_{etb}^{\mathrm{ch},\downarrow} \leqslant p_b^{\max} - \overline{ch}_{etb}, \quad \forall\ e, t, b \tag{17}$$

$$\overline{r}_{etb}^{\mathrm{dis},\downarrow} \leqslant \overline{dis}_{etb}, \quad \forall\ e, t, b \tag{18}$$

$$r_{etb}^{\mathrm{ch},\uparrow}, r_{etb}^{\mathrm{dis},\uparrow}, r_{etb}^{\mathrm{ch},\downarrow}, r_{etb}^{\mathrm{dis},\downarrow} \geqslant 0, \quad \forall\ e, t, b \tag{19}$$

where $\Xi_{\mathrm{UL}} = \{IC, P^{\mathrm{E}}, P^{\mathrm{R}}, \overline{ch}_{etb}, \overline{dis}_{etb}, SoC_b^{\max}, p_b^{\max}, \overline{r}_{etb}^{\mathrm{ES},\downarrow}, \overline{r}_{etb}^{\mathrm{ES},\uparrow}\}$.

Eq. (1) is the objective function that maximizes the expected lifetime profit of the ES units installed, i.e. the difference between the expected lifetime profit collected in the energy and reserve markets, as given in (2) and (3), and the investment cost computed in (4). The budget constraint is enforced in (5), while (6) enforces that the expected lifetime ES profit is sufficient to satisfy a desired rate-of-return. The energy-to-power ration of ES is enforced in (7). The energy state of charge dynamic is modeled in (8), while (9) and (10) enforce the maximum and minimum state of charge limits. Note that (9) and (10) also define the ability of each ES unit to provide up and down reserve services by adding variables $\overline{r}_{etb}^{\mathrm{ES},\uparrow}$ and $\overline{r}_{etb}^{\mathrm{ES},\downarrow}$ to SoC_{etb}. Eqs. (11) and (12) model the state of charge of ES at the beginning and at the end of each characteristic day. The reserve provision by each ES unit is further modeled in (13)–(19). The total up reserve provision by each ES unit is computed in (13) and includes two terms, $\overline{r}_{etb}^{\mathrm{ch},\uparrow}$ and $\overline{r}_{etb}^{\mathrm{dis},\uparrow}$, denoting the upward reserve available in charging and discharging states, respectively. The up reserve provision in the charging state is constrained by the scheduled charging power, i.e. the ES unit provides up reserve by stopping the charging process scheduled in the energy market, as given in (14). In the discharging state, the up reserve provision is given in (15) and limited by the power rating of the ES unit and the discharging schedule in the energy market. Eqs. (16)–(18) model the down reserve provision similarly to the upward reserve in (13)–(15). Eq. (19) imposes non-negativity on the reserve variables.

Note that the profits computed in Eqs. (2) and (3) use the energy and reserve capacity *cleared* by the market operator ($ch_{etb}, dis_{etb}, r_{etb}^{\mathrm{ES},\uparrow}, r_{etb}^{\mathrm{ES},\downarrow}$), while the ES operations constrained by Eqs. (7)–(19) are based on the *offered* energy and reserve capacity ($\overline{ch}_{etb}, \overline{dis}_{etb}, \overline{r}_{etb}^{\mathrm{ES},\uparrow}, \overline{r}_{etb}^{\mathrm{ES},\downarrow}$). This difference makes it possible to realistically estimate the revenue of the ES investor and, therefore, make adequate investment decisions, while ensuring that all offered capacity can be technically delivered, if cleared by the market.

The presented battery model (1)–(19) does not include degradation costs as they are implicitly included in ES installation costs, Eq. (4). Annualized ES installation costs C^{SoC} and C^{p} are calculated for a specific ES investment cost, ES lifetime and interest rate. After the end of ES life, zero residual value is assumed. ES lifetime is assumed considering the expected number of cycles per day and overall number of cycles the ES can perform.

2.3. LL problem

The wholesale market operation for each characteristic day is modeled as follows:

$$\max_{\Xi_{\mathrm{PLL}}} SW_e = \min_{\Xi_{\mathrm{PLL}}} OC_e = \sum_{t,i} (C_i^{\mathrm{g}}\cdot p_{eti}^{\mathrm{g}} + C_i^{\mathrm{g},\uparrow}\cdot r_{eti}^{\mathrm{g},\uparrow} + C_i^{\mathrm{g},\downarrow}\cdot r_{eti}^{\mathrm{g},\downarrow}) + \sum_{t,b} (C_b^{\mathrm{dis}}\cdot dis_{etb} - C_b^{\mathrm{ch}}\cdot ch_{etb} + C_b^{\mathrm{ES},\uparrow}\cdot r_{etb}^{\mathrm{ES},\uparrow} + C_b^{\mathrm{ES},\downarrow}\cdot r_{etb}^{\mathrm{ES},\downarrow}) \tag{20}$$

subject to:

$$\sum_{i\in I_b} p_{eti}^{\mathrm{g}} - \sum_{l|o(l)=b} p_{etl}^{\mathrm{f}} + \sum_{l|r(l)=b} p_{etl}^{\mathrm{f}} + (P_{etb}^{\mathrm{wf}} - p_{etb}^{\mathrm{ws}}) - ch_{etb} + dis_{etb} = D_{etb}: (\lambda_{etb}), \quad \forall\ t, b \tag{21}$$

$$p_{etl}^{\mathrm{f}} = \frac{1}{X_l}(\theta_{eto(l)} - \theta_{etr(l)}): (\xi_{etl}), \quad \forall\ t, l \tag{22}$$

$$-\overline{P}_l^{\mathrm{f}} \leqslant p_{etl}^{\mathrm{f}} \leqslant \overline{P}_l^{\mathrm{f}}: (\underline{\delta}_{etl}, \overline{\delta}_{etl}), \quad \forall\ t, l \tag{23}$$

$$0 \leqslant p_{etb}^{\mathrm{ws}} \leqslant P_{etb}^{\mathrm{wf}}: (\underline{\gamma}_{etb}, \overline{\gamma}_{etb}), \quad \forall\ t, b \tag{24}$$

$$(p_{eti}^{\mathrm{g}} + r_{eti}^{\mathrm{g},\uparrow}) - (p_{e,t-1,i}^{\mathrm{g}} - r_{e,t-1,i}^{\mathrm{g},\downarrow}) \leqslant RU_i: (\overline{\beta}_{eti}), \quad \forall\ t, i \tag{25}$$

$$-(p^{g}_{eti}-r^{g,\downarrow}_{eti}) + (p^{g}_{e,t-1,i} + r^{g,\uparrow}_{e,t-1,i}) \leqslant RD_i : (\underline{\beta}_{eti}), \quad \forall\, t,\, i \tag{26}$$

$$p^{g}_{eti} + r^{g,\uparrow}_{eti} \leqslant \overline{G}_i : (\overline{\alpha}_{eti}), \quad \forall\, t,\, i \tag{27}$$

$$p^{g}_{eti}-r^{g,\downarrow}_{eti} \geqslant 0 : (\underline{\alpha}_{eti}), \quad \forall\, t,\, i \tag{28}$$

$$0 \leqslant r^{g,\uparrow}_{eti} \leqslant \overline{R}^{g,\uparrow}_{eti} : (\underline{\epsilon}^{g,\uparrow}_{eti},\, \overline{\epsilon}^{g,\uparrow}_{eti}), \quad \forall\, t,\, i \tag{29}$$

$$0 \leqslant r^{g,\downarrow}_{eti} \leqslant \overline{R}^{g,\downarrow}_{eti} : (\underline{\epsilon}^{g,\downarrow}_{eti},\, \overline{\epsilon}^{g,\downarrow}_{eti}), \quad \forall\, t,\, i \tag{30}$$

$$\sum_{i\in I} r^{g,\uparrow}_{eti} + \sum_{b\in B} r^{ES,\uparrow}_{etb} \geqslant R^{UP}_{et} : (\lambda^{r,\uparrow}_{et}), \quad \forall\, t \tag{31}$$

$$\sum_{i\in I} r^{g,\downarrow}_{eti} + \sum_{b\in B} r^{ES,\downarrow}_{etb} \geqslant R^{DN}_{et} : (\lambda^{r,\downarrow}_{et}), \quad \forall\, t \tag{32}$$

$$0 \leqslant ch_{etb} \leqslant \overline{ch}_{etb} : (\underline{\epsilon}^{ch}_{etb},\, \overline{\epsilon}^{ch}_{etb}), \quad \forall\, t,\, b \tag{33}$$

$$0 \leqslant dis_{etb} \leqslant \overline{dis}_{etb} : (\underline{\epsilon}^{dis}_{etb},\, \overline{\epsilon}^{dis}_{etb}), \quad \forall\, t,\, b \tag{34}$$

$$0 \leqslant r^{ES,\uparrow}_{etb} \leqslant \overline{r}^{ES,\uparrow}_{etb} : (\underline{\epsilon}^{ES,\uparrow}_{etb},\, \overline{\epsilon}^{ES,\uparrow}_{etb}), \quad \forall\, t,\, b \tag{35}$$

$$0 \leqslant r^{ES,\downarrow}_{etb} \leqslant \overline{r}^{ES,\downarrow}_{etb} : (\underline{\epsilon}^{ES,\downarrow}_{etb},\, \overline{\epsilon}^{ES,\downarrow}_{etb}), \quad \forall\, t,\, b \tag{36}$$

where $\Xi_{PLL} = \{p^{g}_{eti}, p^{f}_{etl}, \theta_{etb}, p^{ws}_{etb}, dis_{etb}, ch_{etb}, r^{g,\uparrow}_{eti}, r^{g,\downarrow}_{eti}, r^{ES,\uparrow}_{etb}, r^{ES,\downarrow}_{etb}\}$.

The market clearing objective given in (20) is to maximize the expected system-wide welfare over a set of characteristic days, which is equivalent to minimizing the system-wide operating cost under the invoked assumption of the inelastic demand. The expected operating cost includes the cost of energy and reserve offers submitted by conventional generators and the cost of energy and reserve bids and offers submitted by the merchant ES investor. The nodal active power balance is enforced in (21). The active power flows are computed in (22) and limited in (23). The available wind power output can be curtailed as in (24). The dispatch model of conventional generators is as follows: (25) and (26) enforce up and down ramping limits, (27) and (28) account for the minimum and maximum power output limits, while (29) and (30) may be used to limit the up and down reserve provision of a generator, e.g. in order to avoid having flexible generators providing only reserve. The up and down reserve requirements are enforced in (31) and (32). The cleared energy and reserve offers of the ES units are accounted for in (33)–(36). Note that dual variables are given in line with respective LL constraints after a colon.

3. Single-level model

As explained in [22], the bilevel model in Section 2 can be converted into a single-equivalent MILP using the KKT optimality conditions of the primal LL problem, strong duality condition between the primal and dual LL problems, and some linearization techniques. Section 3 details these steps.

3.1. KKT optimality conditions

The KKT optimality conditions are given as:

$$\text{Eqs.(21)-(22)} \tag{37}$$

$$\lambda_{etb(i)}-\overline{\beta}_{eti} + \overline{\beta}_{e,t+1,i} + \underline{\beta}_{eti}-\underline{\beta}_{e,t+1,i} - \overline{\alpha}_{eti} + \underline{\alpha}_{eti} = C^{g}_{i} : (p^{g}_{eti})\ \forall\, i,\, t = 1 \ldots n_T-1 \tag{38}$$

$$-\overline{\beta}_{eti}-\underline{\beta}_{e,t+1,i}-\overline{\alpha}_{eti} + \underline{\epsilon}^{g,\uparrow}_{eti}-\overline{\epsilon}^{g,\uparrow}_{eti} + \lambda^{r,\uparrow}_{et} = C^{g,\uparrow}_{i} :(r^{g\uparrow}_{eti}),\ \forall\, t,\, i \tag{39}$$

$$-\overline{\beta}_{e,t+1,i}-\underline{\beta}_{eti}-\underline{\alpha}_{eti} + \underline{\epsilon}^{g,\downarrow}_{eti}-\overline{\epsilon}^{g,\downarrow}_{eti} + \lambda^{r,\downarrow}_{et} = C^{g,\downarrow}_{i} :(r^{g\downarrow}_{eti}), \quad \forall\, t,\, i \tag{40}$$

$$\lambda_{etb} + \underline{\epsilon}^{dis}_{etb}-\overline{\epsilon}^{dis}_{etb} = C^{dis}_{b} : (dis_{etb}), \quad \forall\, t,\, b \tag{41}$$

$$-\lambda_{etb} + \underline{\epsilon}^{ch}_{etb}-\overline{\epsilon}^{ch}_{etb} = -C^{ch}_{b} : (ch_{etb}), \quad \forall\, t,\, b \tag{42}$$

$$\underline{\epsilon}^{ES,\uparrow}_{etb}-\overline{\epsilon}^{ES,\uparrow}_{etb} + \lambda^{r,\uparrow}_{et} = C^{ES,\uparrow}_{b} : (r^{ES,\uparrow}_{etb}), \quad \forall\, t,\, b \tag{43}$$

$$\underline{\epsilon}^{ES,\downarrow}_{etb}-\overline{\epsilon}^{ES,\downarrow}_{etb} + \lambda^{r,\downarrow}_{et} = C^{ES,\downarrow}_{b} : (r^{ES,\downarrow}_{etb}), \quad \forall\, t,\, b \tag{44}$$

$$-\lambda_{eto(l)} + \lambda_{etr(l)}-\xi_{etl} + \underline{\delta}_{etl}-\overline{\delta}_{etl} = 0 : (p^{f}_{etl}), \quad \forall\, t,\, l \tag{45}$$

$$\sum_{l|o(l)\equiv b} \frac{\xi_{etl}}{X_l} - \sum_{l|r(l)\equiv b} \frac{\xi_{etl}}{X_l} = 0 : (\theta_{etb}), \quad \forall\, t,\, b \tag{46}$$

$$-\lambda_{etb} + \underline{\gamma}_{etb}-\overline{\gamma}_{etb} = 0 : (p^{ws}_{etb}), \quad \forall\, t,\, b \tag{47}$$

$$0 \leqslant (p^{f}_{etl} + \overline{P}^{f}_{l}) \perp \underline{\delta}_{etl} \geqslant 0, \quad \forall\, t,\, l \tag{48}$$

$$0 \leqslant (\overline{P}^{f}_{l}-p^{f}_{etl}) \perp \overline{\delta}_{etl} \geqslant 0, \quad \forall\, t,\, l \tag{49}$$

$$0 \leqslant p^{ws}_{etb} \perp \underline{\gamma}_{etb} \geqslant 0, \quad \forall\, t,\, b \tag{50}$$

$$0 \leqslant (P^{wf}_{etb}-p^{ws}_{etb}) \perp \overline{\gamma}_{etb} \geqslant 0, \quad \forall\, t,\, b \tag{51}$$

$$0 \leqslant (RU_i-p^{g}_{eti}-r^{g,\uparrow}_{eti} + p^{g}_{e,t-1,i}-r^{g,\downarrow}_{e,t-1,i}) \perp \overline{\beta}_{eti} \geqslant 0, \quad \forall\, t,\, i \tag{52}$$

$$0 \leqslant (RD_i + p^{g}_{eti}-r^{g,\downarrow}_{eti}-p^{g}_{e,t-1,i}-r^{g,\uparrow}_{e,t-1,i}) \perp \underline{\beta}_{eti} \geqslant 0, \quad \forall\, t,\, i \tag{53}$$

$$0 \leqslant (\overline{G}_i-p^{g}_{eti}-r^{g,\uparrow}_{eti}) \perp \overline{\alpha}_{eti} \geqslant 0, \quad \forall\, t,\, i \tag{54}$$

$$0 \leqslant (p^{g}_{eti}-r^{g,\downarrow}_{eti}) \perp \underline{\alpha}_{eti} \geqslant 0, \quad \forall\, t,\, i \tag{55}$$

$$0 \leqslant r^{g,\uparrow}_{eti} \perp \underline{\epsilon}^{g,\uparrow}_{eti} \geqslant 0, \quad \forall\, t,\, i \tag{56}$$

$$0 \leqslant (\overline{R}^{g,\uparrow}_{eti}-r^{g,\uparrow}_{eti}) \perp \overline{\epsilon}^{g,\uparrow}_{eti} \geqslant 0, \quad \forall\, t,\, i \tag{57}$$

$$0 \leqslant r^{g,\downarrow}_{eti} \perp \underline{\epsilon}^{g,\downarrow}_{eti} \geqslant 0, \quad \forall\, t,\, i \tag{58}$$

$$0 \leqslant (\overline{R}^{g,\downarrow}_{eti}-r^{g,\downarrow}_{eti}) \perp \overline{\epsilon}^{g,\downarrow}_{eti} \geqslant 0, \quad \forall\, t,\, i \tag{59}$$

$$0 \leqslant \left(\sum_{i\in I} r^{g,\uparrow}_{eti} + \sum_{b\in B} r^{ES,\uparrow}_{etb} - R^{UP}_{et}\right) \perp \lambda^{r,\uparrow}_{et} \geqslant 0, \quad \forall\, t \tag{60}$$

$$0 \leqslant \left(\sum_{i\in I} r^{g,\downarrow}_{eti} + \sum_{b\in B} r^{ES,\downarrow}_{etb} - R^{DN}_{et}\right) \perp \lambda^{r,\downarrow}_{et} \geqslant 0, \quad \forall\, t \tag{61}$$

$$0 \leqslant ch_{etb} \perp \underline{\epsilon}^{ch}_{etb} \geqslant 0, \quad \forall\, t,\, b \tag{62}$$

$$0 \leqslant (\overline{ch}_{etb}-ch_{etb}) \perp \overline{\epsilon}^{ch}_{etb} \geqslant 0, \quad \forall\, t,\, b \tag{63}$$

$$0 \leqslant dis_{etb} \perp \underline{\epsilon}^{dis}_{etb} \geqslant 0, \quad \forall\, t,\, b \tag{64}$$

$$0 \leqslant (\overline{dis}_{etb}-dis_{etb}) \perp \overline{\epsilon}^{dis}_{etb} \geqslant 0, \quad \forall\, t,\, b \tag{65}$$

$$0 \leqslant r^{ES,\uparrow}_{etb} \perp \underline{\epsilon}^{ES,\uparrow}_{etb} \geqslant 0, \quad \forall\, t,\, b \tag{66}$$

$$0 \leqslant (\overline{r}^{ES,\uparrow}_{etb}-r^{ES,\uparrow}_{etb}) \perp \overline{\epsilon}^{ES,\uparrow}_{etb} \geqslant 0, \quad \forall\, t,\, b \tag{67}$$

$$0 \leqslant r^{ES,\downarrow}_{etb} \perp \underline{\epsilon}^{ES,\downarrow}_{etb} \geqslant 0, \quad \forall\, t,\, b \tag{68}$$

$$0 \leqslant (\overline{r}^{ES,\downarrow}_{etb}-r^{ES,\downarrow}_{etb}) \perp \overline{\epsilon}^{ES,\downarrow}_{etb} \geqslant 0, \quad \forall\, t,\, b \tag{69}$$

where (37) lists the primal feasibility constraints, (38)–(47) are the dual feasibility constraints, and (48)–(69) are the complementary slackness conditions.

3.2. Strong duality theorem

The primal LL problem and its dual problem are related via the following strong duality condition:

$$- OC_e = \eta_e + \sum_{t,b} (\overline{\epsilon}_{etb}^{\mathrm{ch}}\ \overline{ch}_{etb} + \overline{\epsilon}_{etb}^{\mathrm{dis}}\ \overline{dis}_{etb} + \overline{\epsilon}_{etb}^{\mathrm{ES},\uparrow}\ \overline{r}_{etb}^{\mathrm{ES},\uparrow} + \overline{\epsilon}_{etb}^{\mathrm{ES},\downarrow}\ \overline{r}_{etb}^{\mathrm{ES},\downarrow}), \quad \forall\ e \tag{70}$$

where $\eta_e = \sum_{t,b} (P_{etb}^{\mathrm{wf}} - D_{etb})\lambda_{etb} + \sum_{t,l} \overline{P}_l^{\mathrm{f}} (\underline{\delta}_{etl} + \overline{\delta}_{etl}) + \sum_{t,b} P_{etb}^{\mathrm{wf}} \overline{\gamma}_{etb}$ $+ \sum_{t,i} (RU_i \overline{\beta}_{eti} + RD_i \underline{\beta}_{eti} + \overline{G}_i \overline{\alpha}_{eti} + R_{eti}^{\mathrm{g},\uparrow}\ \overline{\epsilon}_{eti}^{\mathrm{g},\uparrow} + R_{eti}^{\mathrm{g},\downarrow}\ \overline{\epsilon}_{eti}^{\mathrm{g},\downarrow})$ $- \sum_t (R_{et}^{\mathrm{UP}} \lambda_{et}^{\mathrm{r},\uparrow} + R_{et}^{\mathrm{DN}} \lambda_{et}^{\mathrm{r},\downarrow})$.

3.3. Single-level mixed-integer linear equivalent

The KKT optimality conditions in (37)–(69) can replace the LL problem (20)–(36), thus converting the original bilevel model in the following single-level equivalent:

$$\text{Eq.(1)-(19)} \tag{71}$$

$$\text{Eq.(37)-(69)}, \tag{72}$$

where (71) restates the original UL problem. The single-level equivalent of (71) and (72) is nonlinear due to the product of continuous decision variables in (2) and (3), as well as complementary slackness constraints (48)–(69).

3.3.1. Linearization of (2) and (3)

These nonlinear products can be linearized as follows:

1. The dual feasibility constraints in (41)–(44) are used to replace nonlinear terms $\lambda_{etb} \cdot dis_{etb}$, $\lambda_{etb} \cdot ch_{etb}$, $\lambda_{et}^{\mathrm{r},\uparrow} \cdot r_{etb}^{\mathrm{ES},\uparrow}$, and $\lambda_{et}^{\mathrm{r},\downarrow} \cdot r_{etb}^{\mathrm{ES},\downarrow}$ with products of other continuous lower-level dual variables and continuous lower-level primal variables. For doing that, each term in these constraints has been multiplied by the dual variable of the constraint to obtain the non-linear terms included in (2) and (3) as follows:

$$\lambda_{etb} dis_{etb} = -\underline{\epsilon}_{etb}^{\mathrm{dis}}\ dis_{etb} + \overline{\epsilon}_{etb}^{\mathrm{dis}}\ dis_{etb} + C_b^{\mathrm{dis}} dis_{etb}, \quad \forall\ t,\ b \tag{73}$$

$$\lambda_{etb} ch_{etb} = \underline{\epsilon}_{etb}^{\mathrm{ch}}\ ch_{etb} - \overline{\epsilon}_{etb}^{\mathrm{ch}}\ ch_{etb} + C_b^{\mathrm{ch}} ch_{etb}, \quad \forall\ t,\ b \tag{74}$$

$$\lambda_{et}^{\mathrm{r},\uparrow} r_{etb}^{\mathrm{ES},\uparrow} = -\underline{\epsilon}_{etb}^{\mathrm{ES},\uparrow}\ r_{etb}^{\mathrm{ES},\uparrow} + \overline{\epsilon}_{etb}^{\mathrm{ES},\uparrow}\ r_{etb}^{\mathrm{ES},\uparrow} + C_b^{\mathrm{ES},\uparrow} r_{etb}^{\mathrm{ES},\uparrow}, \quad \forall\ t,\ b \tag{75}$$

$$\lambda_{et}^{\mathrm{r},\downarrow} r_{etb}^{\mathrm{ES},\downarrow} = -\underline{\epsilon}_{etb}^{\mathrm{ES},\downarrow} \cdot r_{etb}^{\mathrm{ES},\downarrow} + \overline{\epsilon}_{etb}^{\mathrm{ES},\downarrow}\ r_{etb}^{\mathrm{ES},\downarrow} + C_b^{\mathrm{ES},\downarrow} r_{etb}^{\mathrm{ES},\downarrow}, \quad \forall\ t,\ b \tag{76}$$

2. Complementary slackness conditions (63)–(69) are used to simplify expressions (73)–(76) in terms of nonlinear products involving continuous lower-level dual variables and continuous upper-level variables. As an example, (73) is simplified considering that term $-\underline{\epsilon}_{etb}^{\mathrm{dis}} \cdot dis_{etb}$ is equal to 0 by constraint (64) and $\overline{\epsilon}_{etb}^{\mathrm{dis}} \cdot dis_{etb} = \overline{\epsilon}_{etb}^{\mathrm{dis}} \cdot \overline{dis}_{etb}$ by constraint (63). Then, Eq. (73) can be reformulated as:

$$\lambda_{etb} dis_{etb} = \overline{\epsilon}_{etb}^{\mathrm{dis}}\ \overline{dis}_{etb} + C_b^{\mathrm{dis}} dis_{etb}, \quad \forall\ t,\ b \tag{77}$$

Following the same procedure with constraints (62) and (63) in (74), (66) and (67) in (75) and (68) and (69) in (76), Eqs. (74)–(76) are recast as:

$$\lambda_{etb} ch_{etb} = -\overline{\epsilon}_{etb}^{\mathrm{ch}}\ \overline{ch}_{etb} + C_b^{\mathrm{ch}} ch_{etb}, \quad \forall\ t,\ b \tag{78}$$

$$\lambda_{et}^{\mathrm{r},\uparrow} r_{etb}^{\mathrm{ES},\uparrow} = \overline{\epsilon}_{etb}^{\mathrm{ES},\uparrow}\ \overline{r}_{etb}^{\mathrm{ES},\uparrow} + C_b^{\mathrm{ES},\uparrow} r_{etb}^{\mathrm{ES},\uparrow}, \quad \forall\ t,\ b \tag{79}$$

$$\lambda_{et}^{\mathrm{r},\downarrow} r_{etb}^{\mathrm{ES},\downarrow} = \overline{\epsilon}_{etb}^{\mathrm{ES},\downarrow}\ \overline{r}_{etb}^{\mathrm{ES},\downarrow} + C_b^{\mathrm{ES},\downarrow} r_{etb}^{\mathrm{ES},\downarrow}, \quad \forall\ t,\ b \tag{80}$$

3. The strong duality equality (70) allows recasting the nonlinear profits (2) and (3) using (77)–(80) as an equivalent linear expression (81):

$$\begin{aligned} P = P^{\mathrm{E}} + P^{\mathrm{R}} = & \\ & \sum_e \pi_e \left(\sum_{b,t} (\lambda_{etb} dis_{etb} - \lambda_{etb} ch_{etb} + \lambda_{et}^{\mathrm{r},\uparrow} r_{etb}^{\mathrm{ES},\uparrow} + \lambda_{et}^{\mathrm{r},\downarrow} r_{etb}^{\mathrm{ES},\downarrow}) \right) = \\ & \sum_e \pi_e \left(\sum_{b,t} (\overline{\epsilon}_{etb}^{\mathrm{dis}}\ \overline{dis}_{etb} + C_b^{\mathrm{dis}} dis_{etb} + \overline{\epsilon}_{etb}^{\mathrm{ch}}\ \overline{ch}_{etb} - C_b^{\mathrm{ch}} ch_{etb} + \overline{\epsilon}_{etb}^{\mathrm{ES},\uparrow}\ \overline{r}_{etb}^{\mathrm{ES},\uparrow} + C_b^{\mathrm{ES},\uparrow} r_{etb}^{\mathrm{ES},\uparrow} + \overline{\epsilon}_{etb}^{\mathrm{ES},\downarrow}\ \overline{r}_{etb}^{\mathrm{ES},\downarrow} + C_b^{\mathrm{ES},\downarrow} r_{etb}^{\mathrm{ES},\downarrow}) \right) = \\ & \sum_e \pi_e \left(-\eta_e - \sum_{t,i} (C_i^{\mathrm{g}} p_{eti}^{\mathrm{g}} + C_i^{\mathrm{g},\uparrow} r_{eti}^{\mathrm{g},\uparrow} + C_i^{\mathrm{g},\downarrow} r_{eti}^{\mathrm{g},\downarrow}) \right) \end{aligned} \tag{81}$$

3.3.2. Linearization of (48)–(69)

These nonlinearities can be handled using the standard Fortuny and McCarl transformation [37]. This transformation is rather commonly used (e.g. in our previous work [14]), and we therefore omit its description.

4. Solution procedure

The single-level MILP equivalent in Section 3.3 cannot be solved efficiently using off-the-shelf solvers (e.g. using a branch-and-cut method), even for relatively small instances, due to a large number of binary variables imposed by the linearized complementary slackness conditions (48)–(69). Instead, this paper applies Benders' decomposition algorithm. Observe that if variables $SoC_b^{\max}$ and $p_b^{\max}$ are fixed to given values, problem (1)–(36) can be decomposed by characteristic days e.

This algorithm is explained in the rest of this section, where superscript (ν) denotes the iteration counter.

4.1. Subproblems

Each subproblem emulates the wholesale market operation for each characteristic day assuming that investment variables $SoC_b^{\max(\mu)}$ and $p_b^{\max(\nu)}$ are fixed (i.e. obtained from the previous execution of the master problem). The solution of the subproblems provides energy and reserve prices and sensitivities of the ES merchant profit. Then, the following problem is solved for each characteristic day e:

$$\left\{ \max_{\Xi_{\mathrm{SP}_e}} \pi_e \left(-\eta_e - \sum_{t,i} (C_i^{\mathrm{g}} p_{eti}^{\mathrm{g}} + C_i^{\mathrm{g},\uparrow} r_{eti}^{\mathrm{g},\uparrow} + C_i^{\mathrm{g},\downarrow} r_{eti}^{\mathrm{g},\downarrow}) \right) \right. \tag{82}$$

subject to:

$$\text{Eq.(8)–(19), (21)–(22), (38)–(69)} \tag{83}$$

$$SoC_b^{\max} = SoC_b^{\max,(\nu)} : (\lambda_{eb}^{S,(\nu)}), \quad \forall\ b \tag{84}$$

$$p_b^{\max} = p_b^{\max,(\nu)} : (\lambda_{eb}^{P,(\nu)}), \quad \forall\ b \}, \quad \forall\ e \tag{85}$$

The optimal objective function of the subproblem associated with characteristic day e in iteration (ν) is denoted by $SP_e^{(\nu)}$, which represents the profit obtained by the merchant ES investor on characteristic day e.

4.2. Master problem

The master problem is a relaxed approximation of the original problem that is solved to determine the ES investment decisions. The formulation of the master problem is:

$$\max_{\Xi_{\mathrm{MP}}} \quad \alpha - IC \tag{86}$$

subject to:

Constraint (5) (87)

$$\alpha \geqslant \chi \cdot IC \tag{88}$$

$$\alpha \leqslant \sum_{e} SP_{e}^{(\nu)} + \sum_{b,e} (\lambda_{eb}^{S,(\nu)} (SoC_{b}^{\max} - SoC_{b}^{\max,(\nu)}) + \lambda_{eb}^{P,(\nu)} (p_{b}^{\max} - p_{b}^{\max,(\nu)})), \quad \forall \nu \tag{89}$$

The Benders' cuts formulated by constraint (89) are used to approximate the objective function (1). Observe that in each iteration (ν) an additional Benders' cut is added to the master problem.

4.3. Upper and lower bounds

Since the master problem is a relaxed version of the original problem, the optimal value of its objective function (86) at each iteration (ν) constitutes an upper bound of the original problem:

$$z_{\mathrm{up}}^{(\nu)} = \alpha^{(\nu)} - \sum_{b \in B} (C^{\mathrm{SoC}} \cdot SoC_{b}^{\max,(\nu)} + C^{\mathrm{P}} \cdot p_{b}^{\max,(\nu)}) \tag{90}$$

Considering that each subproblem is solved for fixed values of the investment variables, a lower bound of the original problem can be computed as follows:

$$z_{\mathrm{down}}^{(\nu)} = \sum_{e \in E} SP_{e}^{(\nu)} - \sum_{b \in B} (C^{\mathrm{SoC}} \cdot SoC_{b}^{\max,(\nu)} + C^{\mathrm{P}} \cdot p_{b}^{\max,(\nu)}) \tag{91}$$

If the difference between the upper and lower bounds is smaller than a pre-specified tolerance the algorithm concludes and the optimal investment decisions are $SoC_{b}^{\max,(\nu)}$ and $p_{b}^{\max,(\nu)}$. If not, the algorithm continues.

4.4. On convexity and convergence

Benders' decomposition cannot guaranty optimality when applied to non-convex problems. However, the objective function in (86) can be convexified if a sufficiently large number of subproblems is considered, as explained in [38]. Indeed, the objective function in (86) includes a summation over a number of characteristic days and thus becomes smoother as more characteristics days are considered and the weight of each single day decreases. This convexification allows for a successful implementation of Benders' decomposition for practical needs, e.g. [39,40]. More details on the implementation, performance and convexity of Benders' decomposition algorithm in investment problems is available [41].

5. Case study

The case study is carried out on the 8-zone ISO New England [23] test system with the modifications reported in [5]. Additional modifications are as follows. The reserve requirement is set based on the (3 + 5)% policy devised by NREL in [42], where reserve should cover at least 3% of the load and 5% of wind generation at each time period. Conventional generators offer their full capacity in the energy market at their incremental cost and in the reserve market at 10% of their incremental cost. The planning horizon is represented by a target year, which is modeled by a set of characteristic days divided into hourly periods. As in [43], the characteristic days and their corresponding weights are selected using the scenario reduction algorithm described in [44]. This algorithm iteratively selects the characteristic days to minimize the probability distance between the original set of 365 days and the reduced one. The algorithm also assigns a weight for each selected characteristic day. Our numerical experiments with different numbers of characteristic days suggest that seven characteristic days are enough to ensure numerical stability of the optimal solution. Therefore, seven characteristic days are considered in the numerical results presented below. In line with the previous studies in [5,14,15,25,10], the planning horizon for ES investments is 10 years and the base case ES capital cost is "\$"500/kW and "\$"20/kWh. Investment costs are annualized based on the capital recovery factor $\frac{r(1+r)^{x}}{(1+r)^{x}-1}$, where the interest rate $r = 5\%$ and the lifetime $x = 20$ years, [45]. Unless stated otherwise, $\gamma_{\mathrm{EP}} = 6$ h, $\chi = 1$, $\mu = 0$, $\tau = 0.25$ h, $\gamma_{0} = 0.4$and $IC^{\max} = 20$M\$. The installed ES units bid and offer in the energy market at "\$"180/MWh and "\$"0/MWh and in the reserve market at "\$"1/MW; these price offers and bids are experimentally chosen to ensure that ES units can consistently be cleared in the electricity market.

All simulations are performed with CPLEX 12.6.1 using a server with ten 2.9 GHz processors and 250 GB of RAM. The optimality gap is set to 0.01% and $\epsilon = |z_{\mathrm{down}}^{(\nu)} - z_{\mathrm{up}}^{(\nu)}| < 0.1\%$.

Table 1
Problem size.

	# constraints	# continuous variables	# binary variables
SL-MI LE	590,765	329,300	130,704
Master problem	21	19	0
Subproblems	84,410	47,058	18,672

5.1. Computational complexity

Table 1 summarizes the size of the problems corresponding to the single-level mixed-integer linear equivalent (SL-MI LE) problem formulated in Section 3.3 and the master problem and the subproblems described in Section 4. The computational complexity arises from a relatively large number of binary variables needed to formulate the SL-MI LE problem. As a result, this problem is very difficult to solve directly. In fact, CPLEX failed to return a feasible solution of the single-level equivalent problem in 24 h. In contrast, the proposed solution procedure based on Benders' decomposition obtains a feasible solution

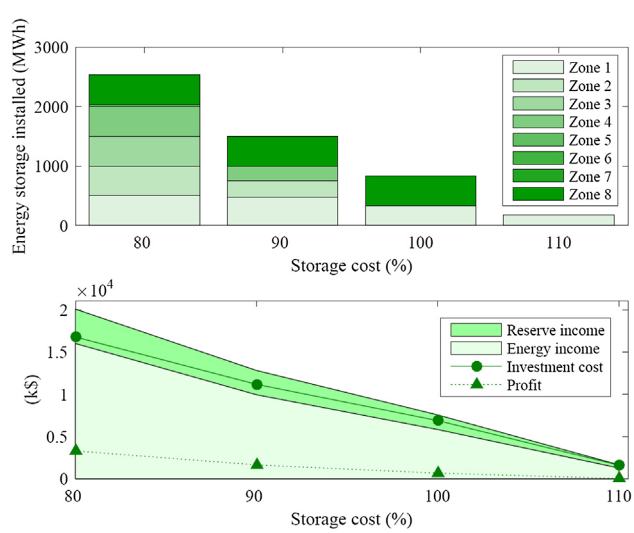

Fig. 2. Storage siting and sizing decisions and cost performance in the joint energy and reserve market. The ES capital cost is in percentage values relative to the base case.

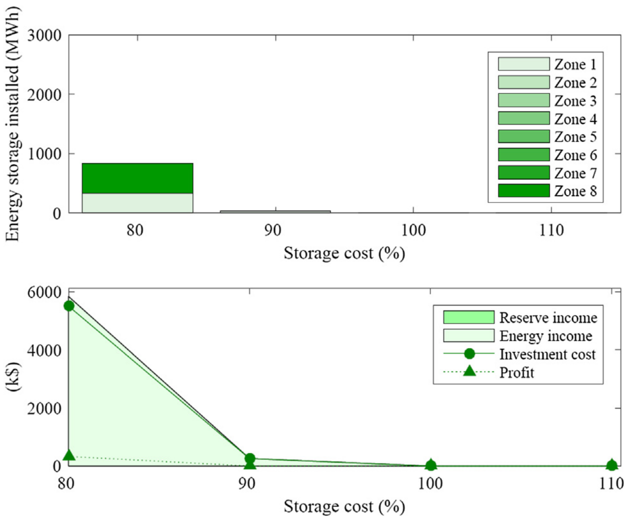

Fig. 3. Storage siting and sizing decisions and cost performance in the energy-only market. The ES capital cost is in percentage values relative to the base case.

with an optimality gap equal to 0.01% in 2.4 h after 16 iterations.

5.2. Energy vs. reserve market

Figs. 2 and 3 compare the optimal siting and sizing decisions for a merchant ES acting in the joint energy and reserve and in the energy-only markets for different values of the ES capital cost. In both cases, the optimal decisions are sensitive to the values of the capital cost scenarios, i.e. the total capacity of ES units installed and the number of locations where the ES units are installed. The notable difference between the two cases is that in the joint energy and reserve market, the ES units are installed for all capital cost scenarios, whereas the energy-only market has sufficient profit opportunities for the two least-cost scenarios only. As a result of fewer profit opportunities in the energy-only market, the total installed capacity of ES units reduces drastically as compared to the joint energy and reserve market. In terms of the cost performance of the merchant ES investor, the joint energy and reserve market is not only more profitable, as expected, but also provides a higher profit margin (the difference between the total revenue and investment cost) than the energy-only market. In both cases, the profit margin increases as the ES capital cost reduces. In the joint energy and reserve market, the profit margin reduces to 0 under the most expensive capital cost scenario, i.e. (6) is binding. The results in Fig. 2 also reveal that the revenue and profit collected by the merchant ES investor in the reserve market is roughly one order of magnitude lower than in the energy market. The difference between the profit obtained in the energy and reserve markets increase, even if the capital cost reduces, i.e. the capital cost is not the primary prohibitor for ES units to participate in the reserve market. Instead, this can be attributed to the market rules, where ES units must oblige to the same requirements as conventional generators.

5.3. Sensitivity analysis

This section studies sensitivity of the ES siting and sizing decisions and their profitability in the joint energy and reserve market, as described in the base case of Section 5.2, relative to most relevant externalities in the proposed model.

5.3.1. Sensitivity to the rate-of-return

The effect of the rate-of-return on decisions made by the merchant ES investor is given in Fig. 4. As the rate-of-return increases relative to the base case in Section 5.2, i.e. the ES investor seeks to achieve a higher profit relative to the investment cost, the total ES capacity installed reduces and the ES locations remain unchanged. Note that increasing the rate-of-return gradually reduces the profit margin, which turns to 0 at $\chi = 1.16$, where (6) becomes binding. Further increasing the rate-of-return makes investing in ES infeasible due to lack of sufficient profit opportunities in the joint energy and reserve market and, therefore, no ES unit is installed in this case ($\chi = 1.18$).

The effect of the rate-of-return on the decisions made by the merchant ES investor if the investment costs of storages is 80% of its nominal value is represented in Fig. 5. As expected, the profit margin increases as the ES capital cost reduces, which allows the merchant ES investor to increase the rate-of-return with respect to the base case.

5.3.2. Sensitivity to the transmission capacity

Fig. 6 illustrates the impact of varying the power flow limits between the zones of the ISO New England test system. Changing the limits around the base case values does not affect the total ES capacity installed, even though some locations can change. As a result, the profit collected by the merchant ES units remains roughly the same. If the limits are reduced below 70% of the base case values, profitability of the merchant ES units drastically increases due to transmission congestion and greater arbitrage opportunities in the electricity market. On the other hand, when the power flow limits are relaxed above 120% of the nominal value, there is no difference in LMPs and there is no sufficient profit opportunities in the joint energy and reserve market to justify merchant investments in ES units. In order to illustrate this result, Fig. 7 presents performance of the optimal investment decisions in the base case (100% transmission line capacity) for different transmission network situations. It is observed that the expected profits obtained by the investor are negative for transmission line capacities greater than or equal to 130%. For this reason, as shown in Fig. 6, if transmission line capacities are high, the investor prefers not to invest in new ES units in order to avoid incurring financial losses.

5.3.3. Sensitivity to the reserve requirement

The effect of changing the reserve requirement is shown in Fig. 8. As the reserve requirement increases, so does the total ES capacity installed. Furthermore, increasing the reserve requirements also increases the number of locations where ES units are profitable. As a result of larger investments, the profit of ES units increases in both the energy and reserve markets. However, this does not yield a significant increase in the total, which essentially remains the same for all values of the reserve requirement sampled in Fig. 8.

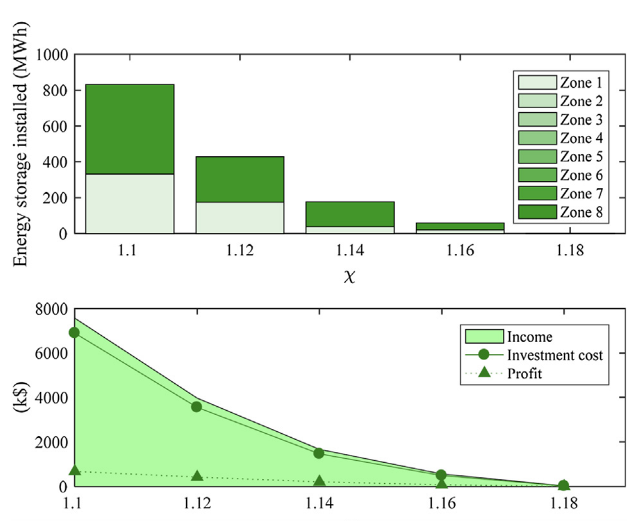

Fig. 4. Impact of the rate-of-return (χ) on the merchant ES investments.

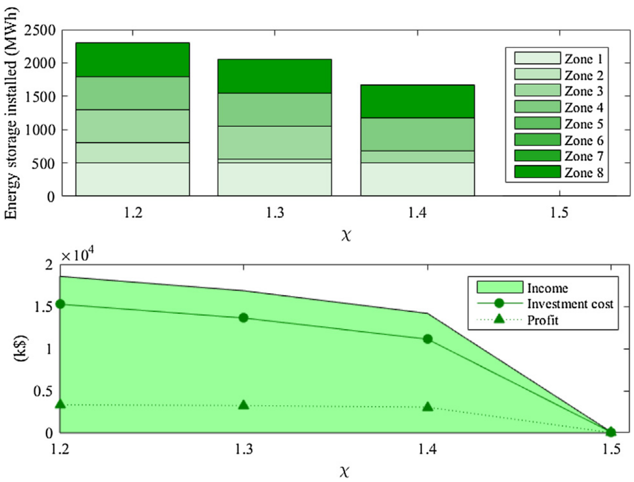

Fig. 5. Impact of the rate-of-return (χ) on the merchant ES investments (80% ES investment cost).

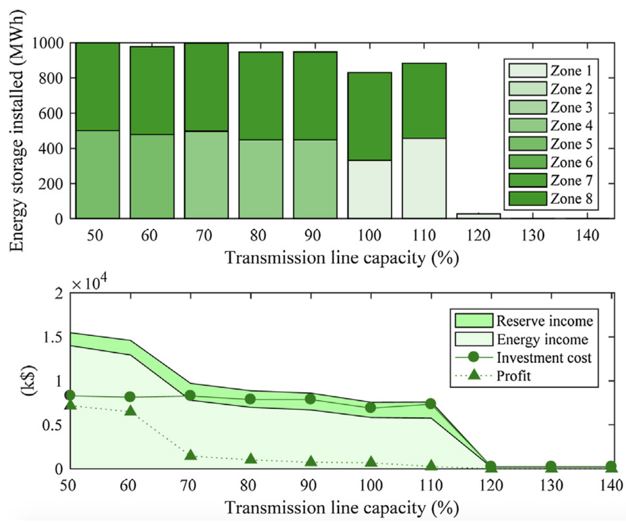

Fig. 6. Storage siting and sizing decisions and cost performance for different values of the power flow limits. The power flow limits are percentage values relative to the base case.

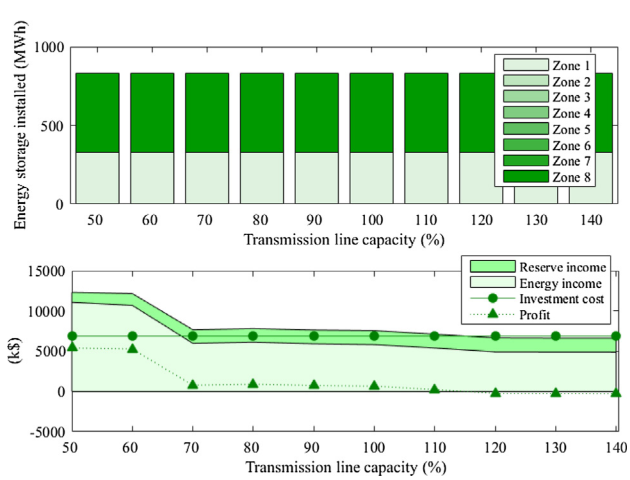

Fig. 7. Storage siting and sizing decisions and cost performance for different values of power flow limits (fixed investment decisions). Transmission line capacity percentages are relative to the base case.

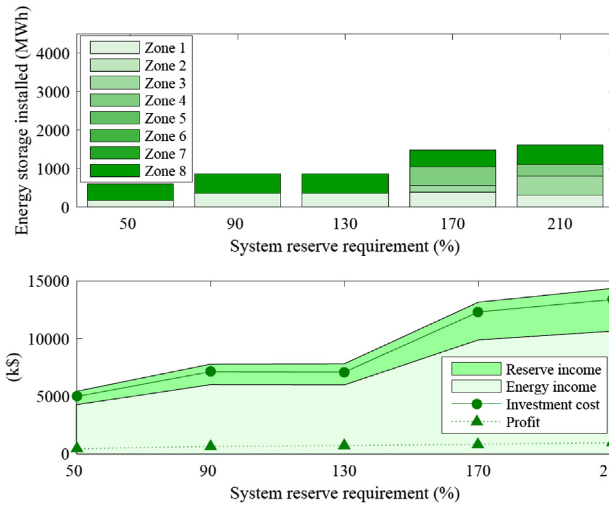

Fig. 8. Storage siting and sizing decisions and cost performance for different system reserve requirements. The percentage values are relative to the base case.

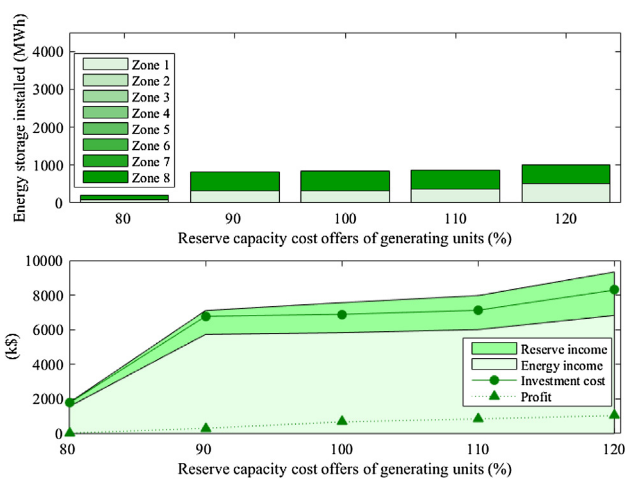

Fig. 9. Storage siting and sizing decisions and cost performance for different reserve capacity cost offers of generating units. The percentage values are relative to the base case.

5.3.4. Sensitivity to the reserve capacity cost offers of generating units

Fig. 9 illustrates the impact of reserve capacity offers of generating units. As a result, the investment decisions remain roughly the same for reserve capacity offer values ranging between 90 and 120% of the nominal values. However, for reserve capacity offer of 80% of the nominal values, ES investments are significantly reduced.

6. Conclusion

This paper presents a bilevel model and a solution technique to optimize merchant investments in ES units participating in the joint energy and reserve market. The proposed model optimizes the siting and sizing decisions of the ES units to maximize their profit opportunities in both markets and ensures a desirable rate-of-return. The case study suggests that participating in the joint energy and reserve market increases profitability of the merchant ES investments. However, the energy market yields higher profits than the reserve market. The sensitivity analysis shows that the siting and sizing decisions and profitability also depend on the transmission limits, penetration levels of renewable generation resources, and reserve requirements.

Acknowledgement

Work of Hrvoje Pandžić has been supported by the Croatian Science Foundation and the Croatian TSO (HOPS) under project Smart Integration of RENewables - SIREN (I-2583-2015) and through European Union's Horizon 2020 research and innovation program under project CROSSBOW - CROSS BOrder management of variable renewable energies and storage units enabling a transnational Wholesale market (Grant No. 773430).

References

[1] Palizban O, Kauhaniemi K. Energy storage systems in modern grids-matrix of technologies and applications. J Energy Storage 2016;6:248–59. https://doi.org/10.1016/j.est.2016.02.001 <http://www.sciencedirect.com/science/article/pii/S2352152X1630010X> .

[2] Castillo A, Gayme DF. Grid-scale energy storage applications in renewable energy integration: A survey. Energy Convers Manage 2014;87:885–94. https://doi.org/10.1016/j.enconman.2014.07.063 <http://www.sciencedirect.com/science/article/pii/S0196890414007018> .

[3] Pandžić H, Wang Y, Qiu T, Dvorkin Y, Kirschen DS. Near-optimal method for siting and sizing of distributed storage in a transmission network. IEEE Trans Power Syst 2015;30(5):2288–300. https://doi.org/10.1109/TPWRS.2014.2364257.

[4] Aneke M, Wang M. Energy storage technologies and real life applications: a state of the art review. Appl Energy 2016;179:350–77. https://doi.org/10.1016/j.apenergy.2016.06.097 <http://www.sciencedirect.com/science/article/pii/S0306261916308728> .

[5] Dvorkin Y, Fernández-Blanco R, Kirschen DS, Pandžić H, Watson JP, Silva-Monroy CA. Ensuring profitability of energy storage. IEEE Trans Power Syst. 2017;32(1):611–23. https://doi.org/10.1109/TPWRS.2016.2563259.

[6] Wogrin S, Gayme DF. Optimizing storage siting, sizing, and technology portfolios in transmission-constrained networks. IEEE Trans Power Syst 2015;30(6):3304–13. https://doi.org/10.1109/TPWRS.2014.2379931.

[7] Dvijotham K, Chertkov M, Backhaus S. Storage sizing and placement through operational and uncertainty-aware simulations. In: 2014 47th Hawaii international conference on system sciences; 2014. p. 2408–16. doi:https://doi.org/10.1109/HICSS.2014.302.

[8] Pudjianto D, Aunedi M, Djapic P, Strbac G. Whole-systems assessment of the value of energy storage in low-carbon electricity systems. IEEE Trans. Smart Grid 2014;5(2):1098–109. https://doi.org/10.1109/TSG.2013.2282039.

[9] Go RS, Munoz FD, Watson J-P. Assessing the economic value of co-optimized grid-scale energy storage investments in supporting high renewable portfolio standards. Appl Energy 2016;183:902–13. https://doi.org/10.1016/j.apenergy.2016.08.134 <http://www.sciencedirect.com/science/article/pii/S030626191631234X> .

[10] Fernández-Blanco R, Dvorkin Y, Xu B, Wang Y, Kirschen DS. Optimal energy storage siting and sizing: a wecc case study. IEEE Trans Sustain Energy 2017;8(2):733–43. https://doi.org/10.1109/TSTE.2016.2616444.

[11] Nasrolahpour E, Kazempour SJ, Zareipour H, Rosehart WD. Strategic sizing of energy storage facilities in electricity markets. IEEE Trans Sustain Energy 2016;7(4):1462–72. https://doi.org/10.1109/TSTE.2016.2555289.

[12] Nasrolahpour E, Zareipour H, Rosehart WD, Kazempour SJ. Bidding strategy for an energy storage facility. In: 2016 Power Systems Computation Conference (PSCC); 2016. p. 1–7. doi:https://doi.org/10.1109/PSCC.2016.7541016.

[13] Krishnan V, Das T. Optimal allocation of energy storage in a co-optimized electricity market: Benefits assessment and deriving indicators for economic storage ventures. Energy 2015;81:175–88. https://doi.org/10.1016/j.energy.2014.12.016 <http://www.sciencedirect.com/science/article/pii/S0360544214013747> .

[14] Dvorkin Y. Can merchant demand response affect investments in merchant energy storage? IEEE Trans Power Syst 2018;33(3):2671–83. https://doi.org/10.1109/TPWRS.2017.2753140.

[15] Dvorkin Y, Fernández-Blanco R, Wang Y, Xu B, Kirschen DS, Pandžić H, et al. Co-planning of investments in transmission and merchant energy storage. IEEE Trans Power Syst 2018;33(1):245–56. https://doi.org/10.1109/TPWRS.2017.2705187.

[16] Pandžić K, Pandžić H, Kuzle I. Coordination of regulated and merchant energy storage investments. IEEE Trans Sustain Energy 2017:1. https://doi.org/10.1109/TSTE.2017.2779404.

[17] Peker M, Kocaman AS, Kara BY. Benefits of transmission switching and energy storage in power systems with high renewable energy penetration. Appl Energy 2018;228:1182–97. https://doi.org/10.1016/j.apenergy.2018.07.008 <http://www.sciencedirect.com/science/article/pii/S0306261918310353> .

[18] Genoese F, Egenhofer C, Hogan M, Redl C, Steigenberger M, Graichen P, et al. The future of the european power market. Intereconomics 2015;50(4):176–97. https://doi.org/10.1007/s10272-015-0541-3.

[19] Domínguez R, Conejo AJ, Carrión M. Investing in generation capacity: a multi-stage linear-decision-rule approach. IEEE Trans Power Syst 2016;31(6):4784–94. https://doi.org/10.1109/TPWRS.2016.2522505.

[20] Dehghan S, Amjady N, Conejo AJ. Adaptive robust transmission expansion planning using linear decision rules. IEEE Trans Power Syst 2017;32(5):4024–34. https://doi.org/10.1109/TPWRS.2017.2652618.

[21] Fertig E, Heggedal AM, Doorman G, Apt J. Optimal investment timing and capacity choice for pumped hydropower storage. Energy Syst 2014;5(2):285–306. https://doi.org/10.1007/s12667-013-0109-x.

[22] Arroyo JM. Bilevel programming applied to power system vulnerability analysis under multiple contingencies. IET Gen Transm Distrib 2010;4(2):178–90. https://doi.org/10.1049/iet-gtd.2009.0098.

[23] Krishnamurthy D, Li W, Tesfatsion L. An 8-zone test system based on iso new England data: development and application. IEEE Trans Power Syst 2016;31(1):234–46. https://doi.org/10.1109/TPWRS.2015.2399171.

[24] Li N, Hedman KW. Economic assessment of energy storage in systems with high levels of renewable resources. IEEE Trans Sustain Energy 2015;6(3):1103–11. https://doi.org/10.1109/TSTE.2014.2329881.

[25] Xu B, Wang Y, Dvorkin Y, Fernández-Blanco R, Silva-Monroy CA, Watson JP, et al. Scalable planning for energy storage in energy and reserve markets. IEEE Trans Power Syst 2017;32(6):4515–27. https://doi.org/10.1109/TPWRS.2017.2682790.

[26] de Sisternes FJ, Jenkins JD, Botterud A. The value of energy storage in decarbonizing the electricity sector. Appl Energy 2016;175:368–79. https://doi.org/10.1016/j.apenergy.2016.05.014 <http://www.sciencedirect.com/science/article/pii/S0306261916305967> .

[27] Lin Y, Johnson JX, Mathieu JL. Emissions impacts of using energy storage for power system reserves. Appl Energy 2016;168:444–56. https://doi.org/10.1016/j.apenergy.2016.01.061 <http://www.sciencedirect.com/science/article/pii/S0306261916300411> .

[28] Pearre NS, Swan LG. Technoeconomic feasibility of grid storage: mapping electrical services and energy storage technologies. Appl Energy 2015;137:501–10. https://doi.org/10.1016/j.apenergy.2014.04.050 <http://www.sciencedirect.com/science/article/pii/S0306261914004036> .

[29] Energy storage association: Facts & figures, < http://energystorage.org/energy-storage/facts-figures > ; 2017.

[30] Terna storage overview, <www.terna.it/engb/azienda/chisiamo/ternastorage.aspx>.

[31] Sidhu AS, Pollitt MG, Anaya KL. A social cost benefit analysis of grid-scale electrical energy storage projects: a case study. Appl Energy 2018;212:881–94. https://doi.org/10.1016/j.apenergy.2017.12.085 <http://www.sciencedirect.com/science/article/pii/S0306261917318068> .

[32] Ondeck AD, Edgar TF, Baldea M. Impact of rooftop photovoltaics and centralized energy storage on the design and operation of a residential chp system. Appl Energy 2018;222:280–99. https://doi.org/10.1016/j.apenergy.2018.03.131 <http://www.sciencedirect.com/science/article/pii/S0306261918304690> .

[33] Hartmann B, Divényi D, Vokony I. Evaluation of business possibilities of energy storage at commercial and industrial consumers – a case study. Appl Energy 2018;222:59–66. https://doi.org/10.1016/j.apenergy.2018.04.005 <http://www.sciencedirect.com/science/article/pii/S0306261918305476> .

[34] McPherson M, Johnson N, Strubegger M. The role of electricity storage and hydrogen technologies in enabling global low-carbon energy transitions. Appl Energy 2018;216:649–61. https://doi.org/10.1016/j.apenergy.2018.02.110 <http://www.sciencedirect.com/science/article/pii/S0306261918302356> .

[35] Makarov YV, Loutan C, Ma J, de Mello P. Operational impacts of wind generation on california power systems. IEEE Trans Power Syst 2009;24(2):1039–50. https://doi.org/10.1109/TPWRS.2009.2016364.

[36] Weibelzahl M. Nodal, zonal, or uniform electricity pricing: how to deal with network congestion. Front Energy 2017;11(2):210–32. https://doi.org/10.1007/s11708-017-0460-z.

[37] Fortuny-Amat J, McCarl B. A representation and economic interpretation of a two-level programming problem. J Oper Res Soc 1981;32(9):783–92. https://doi.org/10.1057/jors.1981.156.

[38] Bertsekas D, Sandell N. Estimates of the duality gap for large-scale separable nonconvex optimization problems. In: 1982 21st IEEE conference on decision and control; 1982. p. 782–5. doi:https://doi.org/10.1109/CDC.1982.268248.

[39] Baringo L, Conejo AJ. Wind power investment: a Benders decomposition approach. IEEE Trans Power Syst 2012;27(1):433–41. https://doi.org/10.1109/TPWRS.2011.2167764.

[40] Nasri A, Kazempour SJ, Conejo AJ, Ghandhari M. Network-constrained AC unit commitment under uncertainty: a benders' decomposition approach. IEEE Trans Power Syst 2016;31(1):412–22. https://doi.org/10.1109/TPWRS.2015.2409198.

[41] Conejo AJ, Baringo L, Kazempour J, Siddiqui AS. Investment in electricity generation and transmission. Springer; 2016.

[42] National renewable energy laboratory: Western wind and solar integration study; 2010. <https://goo.gl/NvUBK8>.

[43] Carrión M, Dvorkin Y, Pandžić H. Primary frequency response in capacity expansion with energy storage. IEEE Trans Power Syst 2018;33(2):1824–35. https://doi.org/10.1109/TPWRS.2017.2735807.

[44] Growe-Kuska N, Heitsch H, Romisch W. Scenario reduction and scenario tree construction for power management problems. In: 2003 IEEE bologna power tech conference proceedings, vol. 3; 2003. p. 7. doi:https://doi.org/10.1109/PTC.2003.1304379.

[45] Steiner H. Engineering economic principles. McGraw-Hill; 1988.